**Journal of Physical and Theoretical Chemistry**
of Islamic Azad University of Iran, 13 (3) 277-288: Fall 2016
(J. Phys. Theor. Chem. IAU Iran)
ISSN 1735-2126

# Quantum Chemical Modeling of 1-(1, 3-Benzothiazol-2-yl)-3-(thiophene-5-carbonyl) thiourea: Molecular structure, NMR, FMO, MEP and NBO analysis based on DFT calculations

Masoome Sheikhi[1,*] and Siyamak Shahab[2]

[1] Young Researchers and Elite Club, Gorgan Branch, Islamic Azad University, Gorgan, Iran
[2] Institute of Physical Organic Chemistry, National Academy of Sciences of Belarus,13 Surganov Str, Minsk 220072, Belarus

Received December 2016; Accepted January 2017

## ABSTRACT

In the present work, the quantum theoretical calculations of the molecular structure of the 1-(1, 3-Benzothiazol-2-yl)-3-(thiophene-5-carbonyl) thiourea has been predicted and are evaluated using Density Functional Theory (DFT) in gas phase. The geometry of the title compound was optimized by B3LYP/6-311+G and B3LYP/6-311+G* methods and the experimental geometrical parameters of the title compound such as bond lengths (Å), bond angles (°) and torsion angels (°) were compared with calculated results. The theoretical $^{1}H$ and $^{13}C$ NMR chemical shift (GIAO method) values of the title compound are calculated and compared with the experimental results. The computed data are in good agreement with the experimental data. Frontier molecular orbitals (FMOs) such as HOMO orbital, LUMO orbital and HOMO-LUMO energy gap, molecular electrostatic potential (MEP), electronic properties such as ionization potential, electron affinity, global hardness, electronegativity, electronic chemical potential, electrophilicity, chemical softness and NBO analysis of the title compound were investigated and discussed by theoretical calculations.

**Keywords:** Thiourea; DFT calculation; Chemical shift; NBO analysis; Electronic properties

# INTRODUCTION

The compound thiourea and its derivatives are a class of organic compounds which playing an important role in coordination chemistry with transition metals. Thioureas are known to exhibit a wide range of biological activities including antiviral, antibacterial, antifungal, antitubercular, antithyroidal, herbicidal, and insecticidal activities [1] and as agrochemicals [2,3]. The thiourea derivatives containing amino functional groups are known as epoxy resin curing agent [4]. In recent years, computational chemistry has become an important tool for chemists and a well-accepted partner for experimental chemistry [5,6]. Density functional theory (DFT) method has become a major tool in the methodological arsenal of computational organic chemists. Javad Farzanfar and et al. [7] investigated the synthesis and theoretical calculations and antibacterial properties of three new thiourea ligands. Theoretical calculations show that the antibacterial activities of

[*]Corresponding author: m.sheikhi2@gmail.com

thiourea ligands have some relation with the LUMO energy and the difference between LUMO and HOMO energies. The compound N-(4-Nitrobenzoyl)-N-(1,5-dimethyl-3-oxo-2-phenyl-1H-3(2H)-pyrazolyl)thiourea hydrate is a novel thiourea compound that it is synthesized by N. Burcu Arslan and et al. [8]. They investigated the crystal structural and energetic characteristics of the title compound by DFT method with the 6-31G* basis set. The results indicate that the experimental vibrational frequencies and chemical shift values are in a good agreement with the results of DFT method. Hamza M. Abosadiya and et al. [9] reported the Synthesis, X-ray, NMR, FT-IR, UV/vis, DFT and TD-DFT studies of N-(4-chlorobutanoyl)-N0-(2-,3-and4-methylphenyl)thiourea derivatives. They detected the intramolecular hydrogen bond in the title compounds. Synthesis of a new compound of 1-(4-methoxyphenyl)-3-(pyridine-3-ylmethyl) thiourea is reported by Md Mushtaque and et al [10]. They studied the molecular conformation, structural parameters, NBO analysis and IR and UV spectra of the title compound using the B3LYP/6-311++G* level of energy. In UV-visible spectroscopy of the title compound, the experimental and theoretical transitions are good agreement with each other. Diego M. Gil [11] investigated molecular structure, spectroscopic (IR, Raman, UV-Vis), NBO and HOMO-LUMO analysis of 1-benzyl-3-(2-furoyl) thiourea by using quantum chemical studies. According to their results, the calculated geometrical parameters of the title are in good agreement with the X-ray results. Using NBO analysis the stability of the title compound arising from hyperconjugative interaction and charge delocalization has been analyzed. Sohail Saeed and et al. [12,13] have reported synthesis of the compound 1-(1, 3-Benzothiazol-2-yl)-3-(thiophene-5-carbonyl) thiourea and was confirmed by single-crystal X-ray analysis [14]. In the present work, we investigate the energetic and structural properties of crystal structure 1-(1, 3-Benzothiazol-2-yl)-3-(thiophene-5-carbonyl) thiourea using the DFT/B3LYP method with 6-311+G and 6-311+G* basis sets. The optimized geometry, frontier molecular orbitals (FMO), detail of quantum molecular descriptors, molecular electrostatic potential (MEP), natural charge and NBO analysis of the title compound were calculated.

## COMPUTATIONAL METHODS

In this work, we have carried out quantum theoretical calculations and has optimized structure of the compound 1-(1,3-Benzothiazol-2-yl)-3-(thiophene-5-carbonyl) thiourea using the DFT/B3LYP [15] method with 6-311+G and 6-311+G* basis sets by the Gaussian 09W program package [16] in gas phse. The electronic properties such as $E_{HOMO}$, $E_{LUMO}$, HOMO-LUMO energy gap and dipole moment ($\mu_D$) were calculated [17]. The optimized molecular structure, HOMO and LUMO surfaces were visualized using GaussView 05 program [18]. We calculated NMR parameters such as $^{1}H$ and $^{13}C$ chemical shift [17] for the title structure using B3LYP/6-311+G and B3LYP/6-311+G* methods. The electronic structure of the title compound was studied by using Natural Bond Orbital (NBO) analysis [19] using B3LYP/6-311+G* level of energy in order to understand hyperconjugative interactions and charge delocalization.

## RESULTS AND DISCUSSION

### *Optimized geometry*

The optimized geometry of 1-(1, 3-Benzothiazol-2-yl)-3-(thiophene-5-carbonyl) thiourea is performed by DFT/B3LYP method with 6-311+G and 6-311+G* basis sets (Fig. 1(b)).

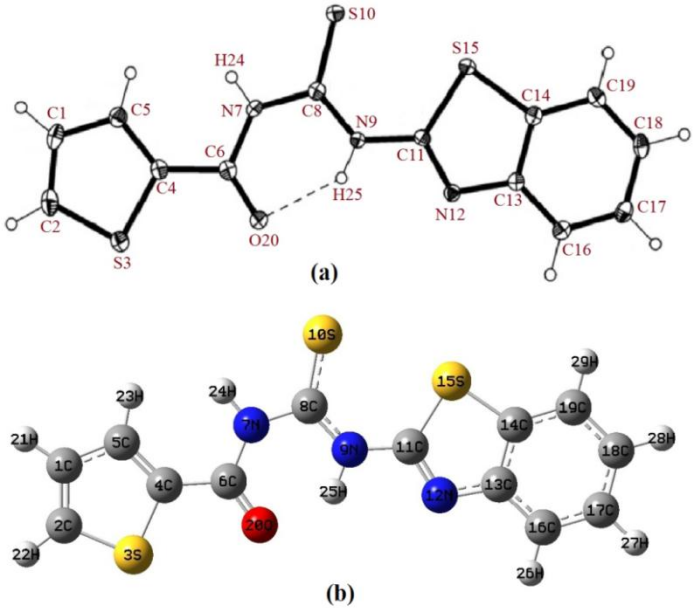


**Fig. 1.** X-Ray crystal structure of the title compound (a); The theoretical geometric structure of the title compound (optimized using the B3LYP/6-311+G* level) (b).

The selected experimental and calculated geometrical parameters of the title compound such as bond lengths (Å), bond angles (°) and torsion angels (°) have been obtained by B3LYP/6-311+G* and B3LYP/6-311+G methods are listed in Table 1. As can be seen in Table 1, the calculated parameters show good approximation and can be used as a foundation to calculate the other parameters for the title compound.

According to Table 1, the average differences of the theoretical parameters from the experimental for bond lengths of the title compound were found to be low. We found that most of the calculated bond lengths are slightly longer than X-ray values that it is due to the fact that experimental result corresponds to interacting molecules in the crystal lattice, whereas computational method deals with an isolated molecule in gaseous phase [14]. The calculated C8-S10 bond length of C=S group by 6-311+G and 6-311+G* basis sets is 1.712Å and 1.666Å respectively, which are in good agreement with experimental value (1.665Å). The normal single C–N bond length is 1.475Å. As can be seen in Table 2, the C–N bond lengths in X-ray and optimized structure of the title compound are shorter than the normal single C–N bond length, that is due to conjugation effect of nitrogen atom with phenyl ring, C=O and C=S groups. The bond angel of C14-C13-C16 in the X-ray structure is 120.14°, while the calculated bond angle by 6-311+G and 6-311+G* basis sets is 119.52° and 119.84° respectively, therefore they are close to the typical hexagonal angle of 120° for $sp^2$ hybridization. In the thiophene ring, the bond angle at the sulphur is around 93°, the C-C-S angle is around 109° and the other two carbons have a bond angle around 114°. The bond angel of C2-S3-C4 in the X-ray and by 6-311+G and 6-311+G* basis sets is 91.67°, 91.12° and 89.20° respectively, which they are close to the typical 93° due to angle strain in thiophene ring. According to experimental results, the dihedral angles C4-C6-N7-C8 and C8-N9-C11-N12 are 179.12° and

174.31°, therefore thiourea group (HN-CS- NH) in the title compound is planar.

**Table 1.** Selected optimized geometrical parameters of the title compound calculated by B3LYP method with 6-311+G* ans 6-311+G basis sets

| Parameter | Experimental[a] | B3LYP/6-311+G* | B3LYP/6-311+G |
|---|---|---|---|
| **Bond lengths(Å)** | | | |
| C1-C2 | 1.362(19) | 1.371 | 1.367 |
| C1-C5 | 1.408(17) | 1.416 | 1.426 |
| C2-S3 | 1.702(13) | 1.721 | 1.789 |
| S3-C4 | 1.717(12) | 1.743 | 1.810 |
| C4-C5 | 1.380(16) | 1.389 | 1.375 |
| C4-C6 | 1.464(16) | 1.470 | 1.459 |
| C6-N7 | 1.391(15) | 1.388 | 1.391 |
| C6-O20 | 1.225(14) | 1.226 | 1.259 |
| N7-C8 | 1.384(15) | 1.401 | 1.404 |
| C8-N9 | 1.343(15) | 1.353 | 1.356 |
| C8-S10 | 1.665(12) | 1.666 | 1.712 |
| N9-C11 | 1.391(14) | 1.389 | 1.387 |
| C11-N12 | 1.297(14) | 1.295 | 1.301 |
| C11-S15 | 1.753(11) | 1.771 | 1.846 |
| N12-C13 | 1.389(15) | 1.380 | 1.398 |
| C13-C14 | 1.405(16) | 1.411 | 1.411 |
| C13-C16 | 1.402(16) | 1.402 | 1.401 |
| C14-S15 | 1.746(12) | 1.761 | 1.829 |
| C18-C19 | 1.384(17) | 1.390 | 1.397 |
| **Bond angles (°)** | | | |
| C2-C1-C5 | 112.17(11) | 112.23 | 113.36 |
| C2-S3-C4 | 91.67(6) | 91.12 | 89.20 |
| C4-C6-N7 | 113.61(10) | 115.41 | 116.41 |
| N7-C8-N9 | 115.51(10) | 114.72 | 114.84 |
| N7-C8-S10 | 118.87(9) | 118.30 | 117.72 |
| N9-C11-S15 | 125.03(9) | 124.89 | 125.07 |
| C11-S15-C14 | 87.69(5) | 87.43 | 86.04 |
| C11-N12-C13 | 109.79(10) | 110.86 | 112.68 |
| C14-C13-C16 | 120.14(11) | 119.52 | 119.84 |
| C17-C18-C19 | 120.97(11) | 120.88 | 120.87 |
| **Torsion angels (°)** | | | |
| S3-C4-C6-O20 | -6.64(16) | -0.04 | -0.05 |
| S3-C4-C6-N7 | 173.16(8) | 179.94 | 179.93 |
| C4-C6-N7-C8 | 179.12(11) | 179.99 | 179.98 |
| C6-N7-C8-S10 | 179.55(9) | -179.99 | -179.99 |
| C6-N7-C8-N9 | -0.31(18) | 0.01 | 0.01 |
| S10-C8-N9-C11 | -2.33(17) | 0.00 | 0.00 |
| C8-N9-C11-N12 | -174.31(11) | -180.00 | -180.00 |

[a] Taken from Ref. [14].

In addition, the experimental [14] and theoretical values of intramolecular hydrogen bond length of the title compound summarized in Table 2. X-ray diffraction analysis of the title compound shows that the structure is stabilized by intramolecular N9-H25…O20 hydrogen bond (see Fig. 1 (a)). By knowing the bond length, the strength of the hydrogen bond can be determined as very strong (below 2.5Å), strong (2.5-2.7Å), normal (2.7-2.9Å) and weak (above 2.9Å). In intramolecular N9-H25…O20 hydrogen bond, the experimental value of bond length H25…O20 is 0.849Å and the calculated values by B3LYP/6-311+G and B3LYP/6-311+G* methods are 1.815Å and 1.860Å respectively, that suggesting the existence of very strong intramolecular hydrogen bond.

***NMR chemical shift analysis***

In the present study, the theoretical $^{1}H$ and $^{13}C$ NMR chemical shift values of title compound were calculated by B3LYP method with 6-311+G* and 6-311+G basis sets using GIAO method. Then calculated $^{1}H$ and $^{13}C$ NMR chemical shifts compared with the experimental values (Table 3).

$^{1}H$ and $^{13}C$ NMR chemical shifts are reported in ppm relative to TMS. According to results, it can be seen a good agreement between experimental and calculated values. The difference between the theoretical and experimental values may be due to the fact that theoretical calculations of the title compound have been done in gas phase. The aromatic protons in recorded $^{1}H$ NMR appeared at the range of 7.31-8.10 ppm, while the theoretical values by B3LYP/6-311+G* and B3LYP/6-311+G methods appeared at 6.66-7.61 ppm and 6.17-7.01 ppm, respectively. The chemical shifts of the protons of thiourea such as H24 and H25 atoms in experimental $^{1}H$ NMR spectrum appeared at 10.25 and 12.40 ppm, respectively. The calculated chemical shift values of the H24 by 6-311+G* and 6-311+G basis sets appeared at 8.25 ppm and 7.97 ppm and calculated chemical shift values of the H25 by 6-311+G* and 6-311+G basis sets appeared at 11.88 ppm and 12.00 ppm, respectively. The high chemical shift values of the H25 compared with H24 is due to the formation of the N9-H25…O20 intramolecular hydrogen bonding. From experimental $^{13}C$ NMR spectrum it is found that, the carbon chemical shifts of C6 (C=O), C8 (C=S) and C11 (C=N) atoms are found at 168.29 ppm, 179.02 ppm and 172.2 ppm respectively, whereas the calculated chemical shift values of the C6, C8, C11 atoms by B3LYP/6-311+G* method appeared at 162.01 ppm, 182.73 ppm, 166.40 ppm respectively, and by B3LYP/6-311+G method appeared at 162.28 ppm, 185.13 ppm, 165.39 ppm respectively.

**Table 2.** N9-H25…O20 hydrogen-bond geometry (Å) of the title compound (Experimental and calculated by B3LYP method with 6-311+G and 6-311+G* basis sets)

| Parameter | Experimental [a] | B3LYP/6-311+G | B3LYP/6-311+G* |
|---|---|---|---|
| N9-H25(Å) | 0.849(16) | 1.029 | 1.024 |
| H25…O20(Å) | 1.962(16) | 1.815 | 1.860 |
| N9…O20(Å) | 2.665(13) | 2.658 | 2.686 |

[a] Taken from Ref. [14]

**Table 3.** The selected theoretical and experimental $^{1}H$ and $^{13}C$ chemical shifts for the title compound

| Atoms | Experimental [a] (DMSO-$d_6$) | Theoretical (TMS) | |
|---|---|---|---|
| | | B3LYP/6-311+G* | B3LYP/6-311+G |
| $^{1}$HNMR | | | |
| H21 | 7.34 | 6.66 | 6.17 |
| H22 | 7.34 | 7.19 | 6.99 |
| H23 | 7.34 | 6.88 | 6.36 |
| H24 | 10.25 | 8.25 | 7.97 |
| H25 | 12.40 | 11.88 | 12.00 |
| H26 | 8.10 | 7.61 | 7.01 |
| H27 | 7.31 | 7.14 | 6.55 |
| H28 | 7.31 | 7.00 | 6.40 |
| H29 | 8.10 | 7.45 | 6.74 |
| $^{13}$CNMR | | | |
| C1 | 125.7 | 129.77 | 125.08 |
| C2 | - | 145.76 | 156.03 |
| C4 | - | 148.30 | 154.10 |
| C5 | 128.5 | 130.43 | 124.83 |
| C6 | 168.29 | 162.01 | 162.28 |
| C8 | 179.02 | 182.73 | 185.13 |
| C11 | 172.2 | 166.40 | 165.39 |
| C13 | 149.4 | 153.82 | 147.17 |
| C14 | 136.5 | 142.94 | 147.33 |
| C16 | 122.3 | 126.75 | 123.41 |
| C17 | - | 129.60 | 125.91 |
| C18 | - | 127.61 | 125.07 |
| C19 | - | 123.98 | 119.94 |

[a] Taken from Ref. [14].

***Electronic properties***

Quantum chemical methods are important for obtaining information about molecular structure and electrochemical behavior. A frontier molecular orbitals (FMO) analysis [21] was done for the title compound using B3LYP/6-311+G* level of energy in gas phase. The highest occupied molecular orbital (HOMO) can act as an electron donor and the lowest unoccupied molecular orbital (LUMO) can act as the electron acceptor. The high value of $E_{HOMO}$ shows the tendency of the compound to donate electron to acceptor compound with low energy, whereas the low value of $E_{LUMO}$ indicates that the compound accept electrons. The FMO results of the title compound are summarized in Table 4.

**Table 4.** Electronic properties of the title compound calculated by the B3LYP/6-311+G* method

| Property | Value |
|---|---|
| $E_{HOMO}$ (eV) | -6.27 |
| $E_{LUMO}$ (eV) | -2.67 |
| Energy gap (eV) | 3.6 |
| Ionisation potential $I$ (eV) | 6.27 |
| Electron affinity $A$ (eV) | 2.67 |
| Electronegativity ($\chi$) | 4.47 |
| Global hardness ($\eta$) | 1.8 |
| Chemical potential ($\mu$) | -4.47 |
| Global electrophilicity ($\omega$) | 5.55 |
| Chemical softness $S$ ($eV^{-1}$) | 0.55 |
| Dipole moment (Debye) | 4.2835 |

The title compound contains 82 occupied molecular orbital and 408

unoccupied virtual molecular orbital. The shape of two important molecular orbitals of the title compound in gas phase such as HOMO and LUMO orbitals is shown in Fig. 2. As shown in Fig. 2, the positive and negative phase is represented in green and red color respectively and charge transfer is taking place within molecule. The graphic pictures of orbitals show the electron density of HOMO is mainly focused on thiocarbonyl group (C=S) and LUMO of the molecule is mainly localized on the whole. Also the HOMO-LUMO energy gap is a important parameter in determining molecular electrical transport properties and reactivity of the molecules. Increase of the HOMO-LUMO energy gap decreases reactivity of the compound that lead to increase in the stability of the compound. As seen in Table 6, the HOMO-LUMO energy gap (ΔE) of the title compound is 3.6 eV that reflects the chemical activity of the molecule. Total electronic densities of states (DOSs) [22] of the title compound was computed and the calculated energy gap clearly is shown (Fig. 2).

A detail of quantum molecular descriptors of the title compound such as ionization potential ($I$=- $E_{HOMO}$), electron affinity ($A$=- $E_{LUMO}$), global hardness ($\eta=I - A/2$), electronegativity ($\chi=I + A/2$), electronic chemical potential ($\mu=-(I + A)/2$) and electrophilicity ($\omega=\mu^2/2\eta$), chemical softness ($S=1/\eta$) [21] are calculated and are listed in Table 6. The energy of HOMO (-6.27 eV) is directly related to the ionization potential, while the energy of LUMO (-2.67 eV) is related

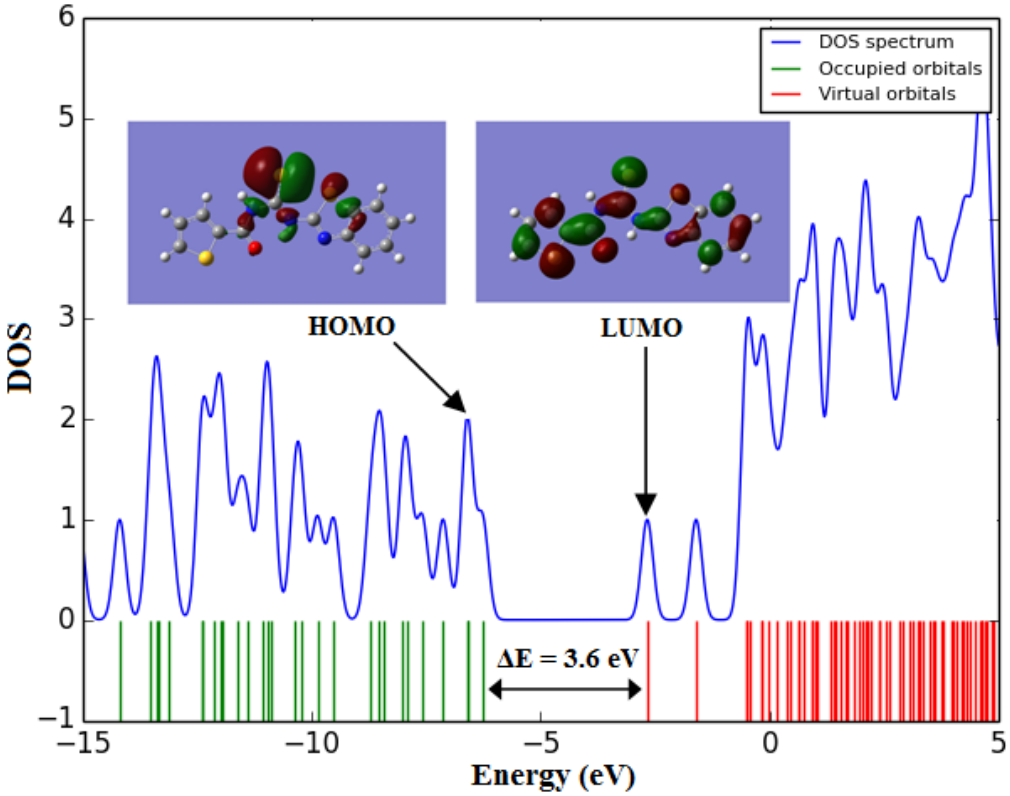


**Fig. 2.** Calculated Frontier molecular orbitals of the title compound DOS plots of the title compound by B3LYP/6-311+G* method.

to the electron affinity. The global hardness ($\eta$) corresponds to the HOMO-LUMO energy gap. A molecule with a small energy gap has high chemical reactivity, low kinetic stability and is a soft molecule, while a hard molecule has a large energy gap [21]. Electronegativity ($\chi$) is a measure of the power of an atom or a group of atoms to attract electrons [23] and the chemical softness ($S$) describes the capacity of an atom or a group of atoms to receive electrons [21]. Dipole moment ($\mu_D$) is a good measure for the asymmetric nature of a structure. The size of the dipole moment depends on the composition and dimensionality of the 3D structures. The calculated dipole moment value shows that the molecule is highly polarity in nature. As shown in Table 6, dipole moment and point group of the title compound is 4.2835 Debye.

***Molecular electrostatic potential (MEP)***

Molecular electrostatic potential (MEP) maps shows the electronic density and are useful in recognition of sites of negative and positive electrostatic potentials for electrophilic attack and nucleophilic reactions as well as hydrogen bonding interactions [24,25]. The difference of the electrostatic potential at the surface are represented by different colors. The negative regions (red, orange and yellow color) of MEP with the high electron density were related to electrophilic reactivity, the positive regions (blue color) with the low electron density ones to nucleophilic reactivity and green color is neutral regions. The MEPs of the title compound was checked out by theoretical calculations using the B3LYP/6-311+G* level of energy (Fig. 3). As shown in Fig. 3, the negative region (red color) of the title compound is mainly focused on phenyl ring and N12 atom. Therefore, these regions are suitable for electrophilic attack. According to MEP map, H24 is the positive potential site therefore it is suitable sites for nucleophilic activity (blue color). The parts of the title compound are pale red, yellow or pale blue. These areas are sites with weak interaction such as S3 (pale blue) and O20 (yellow) atoms. Also the regions with green color indicate areas with zero potential.

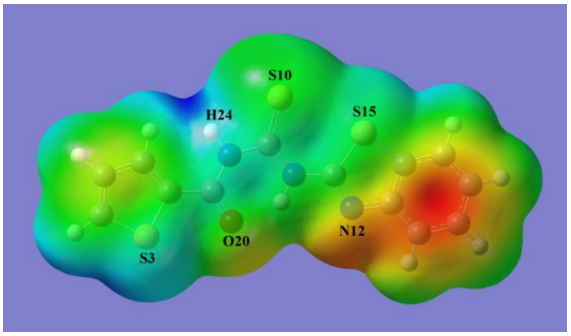


**Fig. 3.** Molecular electrostatic potential (MEP) map of the title compound calculated using the B3LYP/6-311+G* level of energy.

***NBO analysis***

Natural bond orbital (NBO) analysis is important method for studying intra- and inter-molecular bonding and interaction between bonds in molecular systems [26]. Electron donor orbitals, acceptor orbitals and the interacting stabilization energy (E(2)) resulting from the second-order micro disturbance theory are reported in Table 5.

The electron delocalization from filled NBOs (donors) to the empty NBOs (acceptors) describes a conjugative electron transfer process between them. For each donor ($i$) and acceptor ($j$), the stabilization energy E(2) associated with the delocalization $i \rightarrow j$ is estimated [27]:

$$E^{(2)} = \Delta E_{ij} = q_i \frac{F(i,j)^2}{\varepsilon_j - \varepsilon_i} \qquad (2)$$

**Table 5.** Significant donor–acceptor interactions and second order perturbation energies of the compound PAZB-2 calculated using the B3LYP/6-311+G* level of energy

| Donor (i) | Occupancy | Acceptor (j) | Occupancy | E(2)[a] kcal/mol | E(j)-E(i)[b] a.u. | F(i , j)[c] a.u. |
|---|---|---|---|---|---|---|
| π(C1-C2) | 1.82330 | π*(C4-C5) | 0.36351 | 17.85 | 0.29 | 0.067 |
| π(C4-C5) | 1.80991 | π*(C1-C2) | 0.30323 | 14.40 | 0.29 | 0.060 |
| | | π*(C6-O20) | 0.32113 | 21.57 | 0.28 | 0.072 |
| π(C11-N12) | 1.87698 | π*(C13-C14) | 0.47596 | 16.20 | 0.35 | 0.074 |
| π(C13-C14) | 1.63015 | π*(C11-N12) | 0.37898 | 12.12 | 0.25 | 0.049 |
| | | π*(C16-C17) | 0.29996 | 15.97 | 0.30 | 0.063 |
| | | π*(C18-C19) | 0.32120 | 19.36 | 0.29 | 0.068 |
| π(C16-C17) | 1.70518 | π*(C13-C14) | 0.47596 | 20.67 | 0.27 | 0.069 |
| | | π*(C18-C19) | 0.32120 | 19.40 | 0.28 | 0.066 |
| π(C18-C19) | 1.97308 | π*(C13-C14) | 0.47596 | 18.33 | 0.27 | 0.066 |
| | | π*(C16-C17) | 0.29996 | 18.77 | 0.29 | 0.066 |
| π*(C11-N12) | 0.37898 | π*(C13-C14) | 0.47596 | 92.81 | 0.03 | 0.069 |
| π*(C13-C14) | 0.47596 | π*(C16-C17) | 0.29996 | 159.63 | 0.02 | 0.084 |
| | | π*(C18-C19) | 0.32120 | 199.00 | 0.02 | 0.079 |
| | | σ*(C6-O20) | 0.01193 | 1.70 | 1.31 | 0.042 |
| σ(C6-N7) | 1.98646 | σ*(S3-C4) | 0.02673 | 2.14 | 1.05 | 0.042 |
| | | σ*(C8-S10) | 0.1286 | 2.16 | 1.14 | 0.044 |
| σ(C8-N9) | 1.98695 | σ*(N9-C11) | 0.04323 | 2.53 | 1.30 | 0.052 |
| | | σ*(C8-S10) | 0.01286 | 0.58 | 1.17 | 0.023 |
| | | σ*(C11-N12) | 0.01570 | 1.12 | 1.46 | 0.036 |
| σ(C8-S10) | 1.97870 | σ*(C8-N9) | 0.05788 | 1.05 | 1.17 | 0.032 |
| | | σ*(N9-H25) | 0.04782 | 3.02 | 1.10 | 0.052 |
| σ(C11-S15) | 1.97710 | σ*(N9-H25) | 0.04782 | 2.68 | 1.03 | 0.047 |
| | | σ*(C13-C16) | 0.02570 | 0.74 | 1.23 | 0.027 |
| | | σ*(C14-C19) | 0.02096 | 4.34 | 1.24 | 0.065 |
| n1(S3) | 1.98393 | σ*(C1-C2) | 0.01461 | 2.05 | 1.23 | 0.045 |
| | | σ*(C4-C5) | 0.01964 | 2.48 | 1.23 | 0.049 |
| n2(S3) | 1.57994 | π*(C1-C2) | 0.30323 | 24.16 | 0.26 | 0.072 |
| | | π*(C4-C5) | 0.36351 | 22.03 | 0.25 | 0.068 |
| n1(N7) | 1.64543 | π*(C6-O20) | 0.32113 | 57.24 | 0.28 | 0.113 |
| | | π*(C8-S10) | 0.46669 | 57.03 | 0.21 | 0.102 |
| n1(N9) | 1.59382 | π*(C8-S10) | 0.46669 | 84.08 | 0.20 | 0.118 |
| | | π*(C11-N12) | 0.37898 | 42.14 | 0.27 | 0.097 |
| n1(S10) | 1.98392 | σ*(N7-C8) | 0.06239 | 1.90 | 1.09 | 0.041 |
| | | σ*(C8-N9) | 0.05788 | 4.10 | 1.16 | 0.062 |
| | | σ*(C14-S15) | 0.04954 | 0.50 | 0.93 | 0.019 |
| n2(S10) | 1.84582 | σ*(N7-C8) | 0.06239 | 12.85 | 0.58 | 0.079 |
| | | σ*(C8-N9) | 0.05788 | 11.72 | 0.65 | 0.080 |
| | | σ*(C14-S15) | 0.04954 | 3.38 | 0.43 | 0.035 |
| n1(N12) | 1.88339 | σ*(N9-C11) | 0.04323 | 4.79 | 0.77 | 0.055 |
| | | σ*(N9-H25) | 0.04782 | 0.61 | 0.73 | 0.019 |
| | | σ*(C11-S15) | 0.08379 | 16.79 | 0.53 | 0.085 |
| | | σ*(C13-C14) | 0.04077 | 6.21 | 0.91 | 0.068 |
| | | σ*(C13-C16) | 0.02570 | 0.89 | 0.93 | 0.026 |
| n1(S15) | 1.98337 | σ*(C11-N12) | 0.01570 | 2.88 | 1.24 | 0.053 |
| | | σ*(C13-C14) | 0.04077 | 1.78 | 1.21 | 0.042 |
| | | σ*(C14-C19) | 0.02096 | 0.69 | 1.24 | 0.026 |
| n2(S15) | 1.67261 | π*(C11-N12) | 0.37898 | 28.62 | 0.24 | 0.075 |
| | | π*(C13-C14) | 0.47596 | 17.92 | 0.27 | 0.064 |
| n1(O20) | 1.97170 | σ*(C4-C6) | 0.05776 | 1.28 | 1.14 | 0.034 |
| | | σ*(C6-N7) | 0.08244 | 1.89 | 1.11 | 0.041 |
| | | σ*(N9-H25) | 0.04782 | 3.23 | 1.09 | 0.053 |
| n2(O20) | 1.86052 | σ*(C2-S3) | 0.01775 | 0.51 | 0.51 | 0.015 |
| | | σ*(C4-C6) | 0.05776 | 17.33 | 0.71 | 0.101 |
| | | σ*(C6-N7) | 0.08244 | 24.20 | 0.69 | 0.117 |
| | | σ*(N9-H25) | 0.04782 | 8.60 | 0.67 | 0.069 |

[a] E(2) Energy of hyperconjucative interactions,

[b] Energy difference between donor and acceptor i and j NBO orbitals,

[c] F(i, j) Is the Fock matrix element between i and j NBO orbitals.

where $q_i$ is the donor orbital occupancy, $\varepsilon_j$ and $\varepsilon_i$ are diagonal elements and F(i,j) is the off diagonal NBO Fock matrix element. The resonance energy (E(2)) detected the quantity of participation of electrons in the resonance between atoms. The larger E(2) value, the more intensive is the interaction between electron donors and acceptor, i.e. the more donation tendency from electron donors to electron acceptors and the greater the extent of conjugation of the whole system [27]. Delocalization of electron density between occupied Lewis-type (bond or lone pair) NBO orbitals and formally unoccupied (antibond or Rydgberg) non Lewis NBO orbitals correspond to a stabilization donor–acceptor interaction. NBO analysis has been performed for the title compound at the B3LYP/6-311+G* level of energy in order to elucidate the intramolecular, rehybridization and delocalization of electron density within the title compound. The strong, moderate and weak intramolecular hyperconjugative interactions of the title compound such as π→π*, π*→π*, σ→σ*, n→σ* and n→π* transitions are presented in Table 5. According to NBO analysis, the σ(C11-S15)→σ*(C14-C19) transition has the highest resonance energy (4.34 kcal/mol) compared with other σ→σ* transitions of the title compound.

The intramolecular hyperconjugative interactions of the π→π* transitions have the most resonance energy (E(2)) compared with σ→σ* transitions. The important intramolecular hyperconjugative interaction of the π→π* transitions in phenyl ring that lead to a strong delocalization are such as C4-C5→C6-O20 and C13-C14→C16-C17 with the strong resonance energies (E(2)) 21.57 kcal/mol and 20.67 kcal/mol, respectively. The π*→π* transitions have the highest resonance energies compared with other interactions of the title compound. The highest resonance energies of the title compound is observed for π*(C13-C14)→π*(C16-C17) and π*(C13-C14)→π*(C18-C19) transitions with resonance energies (E(2)) 159.63 kcal/mol and 199.00 kcal/mol respectively, that lead to stability of the title compound. The strongest n→π* interactions are due to n1(N7)→σ*(C6-O20), n1(N7)→π*(C8-S10) and n1(N9)→π*(C8-S10) interactions with stabilization energies of 57.24 kcal/mol, 57.03 kcal/mol and 84.08 kcal/mol, respectively. The n1(O20)→σ*(N9-H25) and n2(O20)→σ*(N9-H25) interactions with stabilization energies of 3.23 kcal/mol and 8.60 kcal/mol respectively, show existence of intermolecular hydrogen bond of O20…H25-N9 in the title compound.

## CONCLUSION

In the present study, the electronic structure of the 1-(1, 3-Benzothiazol-2-yl)-3-(thiophene-5-carbonyl) thiourea were modeled using the DFT calculations (B3LYP/6-311+G and B3LYP/6-311+G* levels of energy). From the theoretical and experimental geometric parameters values, it can be seen that experimental values are in good agreement with the theoretical values. The bond length H25…O20 suggesting the existence of very strong intramolecular hydrogen bond. According to results of $^{1}H$ and $^{13}C$ NMR chemical shift, the experimental values are in good agreement with the theoretical values by B3LYP/6-311+G* method. The FMO analysis suggests that charge transfer is taking place within the molecule. From the MEP map, it can be seen that negative region of the title compound is mainly focused on phenyl ring and N12 atom therefore they are suitable sites for electrophilic attack. According to the results of NBO analysis, the n1(O20)→σ*(N9-H25) and

n2(O20)→σ*(N9-H25) interactions show existence of intermolecular hydrogen bond of O20…H25-N9 in the title compound.

## REFERENCES


[1] S. Saeed, M. H. Bhatti, U. Yunus and P. G. Jones, *Acta Crystallogr*. E64 (2008) o1566.

[2] Y. M. Zhang, T. B. Wei, L. Xian and L. M. Gao, *Phosphorus, Sulfur Silicon Relat. Elem*. 179 (2004) 2007.

[3] H. Arslan, N. Duran, G. Borekci, C. K. Ozer and C. Akbay, *Molecules* 14 (2009) 519.

[4] G. Binzet, H. Arslan, U. Florke, N. Kulcu and N. Duran, *J. Coord. Chem*. 59 (2006) 1395.

[5] S. Shahab, H. Alhosseini Almodarresiyeh, R. Kumar and M. Darroudi, *J. Mol. Struct.* 1088 (2015) 105.

[6] S. Shahab, R. Kumar, M. Darroudi and M. Yousefzadeh Borzehandani, *J. Mol. Struct.* 1083 (2015) 198.

[7] J. Farzanfar, K. Ghasemi, A. R. Rezvani, H. Samareh Delarami, A. Ebrahimi, H. Hosseinpoor, A. Eskandari, H. Amiri Rudbari and G. Bruno, *J. Inorg. Biochem.* 147 (2015) 54.

[8] N. Burcu Arslana, C. Kazak and F. Aydin, *Mol. Biomol. Spectrosc.* 89 (2012) 30.

[9] H. M. Abosadiya, E. H. Anouar, S. A. Hasbullah and B. M. Yamin, *Mol. Biomol. Spectrosc.* 144 (2015) 115.

[10] M. Mushtaque, M. Jahan, M. Ali, M. Shahzad Khan, M. Shahid Khan, P. Sahay and A. Kesarwani, *J. Mol. Struct.*1122 (2016) 164.

[11] D. M. Gil, M. E. Defonsi Lestard, O. Estevez-Hernandez, J. Duque and E. Reguera, *Mol. Biomol. Spectrosc.* 145 (2015) 553.

[12] S. Saeed, M. H. Bhatti, U. Youns and P. G. Jones, *Acta Crystallogr*. E64 (2008) o1485.

[13] H. Arslan, U. Florke and N. Kulcu, *J. Chem. Crystallogr*. 33 (2003) 919.

[14] S. Saeed, N. Rashid, P. G. Jones, M. Ali and R. Hussain, *Europ. J. Med Chem.* 45 (2010) 1323.

[15] A. D. Becke, *J. Chem. Phys.* 98 (1993) 5648.

[16] M. J. Frisch, G. W. Trucks, H. B. Schlegel, G. E. Scuseria, M. A. Robb, J. R. Cheeseman, G. Scalmani, V. Barone, B. Mennucci, G. A. Petersson, H. Nakatsuji, M. Caricato, X. Li, H. P. Hratchian, A. F. Izmaylov, J. Bloino, G. Zheng, J. L. Sonnenberg, M. Hada, M. Ehara, K. Toyota, R. Fukuda, J. Hasegawa, M. Ishida, T. Nakajima, Y. Honda, O. Kitao, H. Nakai, T. Vreven, J. A. Montgomery, Jr., J. E. Peralta, F. Ogliaro, M. Bearpark, J. J. Heyd, E. Brothers, K. N. Kudin, V. N. Staroverov, R. Kobayashi, J. Normand, K. Raghavachari, A. Rendell, J. C. Burant, S. S. Iyengar, J. Tomasi, M. Cossi, N. Rega, J. M. Millam, M. Klene, J. E. Knox, J. B. Cross, V. Bakken, C. Adamo, J. Jaramillo, R. Gomperts, R. E. Stratmann, O. Yazyev, A. J. Austin, R. Cammi, C. Pomelli, J. W. Ochterski, R. L. Martin, K. Morokuma, V. G. Zakrzewski, G. A. Voth, P. Salvador, J. J. Dannenberg, S. Dapprich, A. D. Daniels, Ö. Farkas, J. B. Foresman, J. V. Ortiz, J. Cioslowski and D. J. Fox, Gaussian, Inc., Wallingford CT, 2009.

[17] M. Sheikhi, D. Sheikh and A. Ramazani, *S. Afr. J. Chem.* 67 (2014) 151.

[18] A. Frisch, A. B. Nielson and A. J. Holder, GAUSSVIEW User Manual, Gaussian Inc., Pittsburgh, PA, 2000.

[19] M. Sheikhi, E. Balali and H.Lari, *J. Phys. Theor. Chem.* 13 (2016) 155.
[20] B. D. Joshi, P. Tandon and S. Jain, *The Himalayan Physics*. 3 (2012) 44.
[21] M. Sheikhi and D. Sheikh, *Rev. Roum. Chim.* 59 (2014) 761.
[22] A. Ramazani, A. Rouhani, E. Mirhadi, M. Sheikhi, K. Ślepokura and T. Lis, *Nano. Chem. Res.* 1 (2016) 87.
[23] R. G. Parr and W. Yang, *J. Am. Chem. Soc.* 106 (1984) 4049.
[24] D. Habibi, A. R. Faraji, D. Sheikh, M. Sheikhi and S. Abedi, *RSC Adv.* 4 (2014) 47625.
[25] L. Shiri, D. Sheikh and M. Sheikhi, *Rev. Roum. Chim.* 59 (2014) 825.
[26] F. Weinhold and C. R. Landis, Natural Bond Orbitals and Extensions of Localized, 2001.
[27] S. Guidara, A. B. Ahmed, Y. Abid and H. Feki, *Mol. Biomol. Spectrosc.* 127 (2014) 275.